Atomic-Scale Imaging of Wall-by-Wall Breakdown and Concurrent Transport Measurements in Multiwall Carbon Nanotubes

J. Y. Huang,[1,*,†] S. Chen,[1] S. H. Jo,[1] Z. Wang,[1] D. X. Han,[1] G. Chen,[2] M. S. Dresselhaus,[3] and Z. F. Ren[1,*,‡]

[1]*Department of Physics, Boston College, Chestnut Hill, Massachusetts 02467, USA*

[2]*Department of Mechanical Engineering, Massachusetts Institute of Technology, Cambridge, Massachusetts 02139, USA*

[3]*Department of Physics, Electrical Engineering and Computer Science, Massachusetts Institute of Technology, Cambridge, Massachusetts 02139, USA*

(Received 31 March 2005; published 14 June 2005)

We report the atomic-scale imaging with concurrent transport measurements of the breakdown of individual multiwall carbon nanotubes inside a transmission electron microscope equipped with a piezomanipulator. We found unexpectedly three distinct breakdown sequences: namely, from the outermost wall inward, from the innermost wall outward, and alternatively between the innermost and the outmost walls. Remarkably, a significant amount of current drop was observed when an innermost wall is broken, proving unambiguously that every wall is conducting. Moreover, the breakdown of each wall in any sequence initiates in the middle of the nanotube, not at the contact, proving that the transport is not ballistic.

DOI: 10.1103/PhysRevLett.94.236802 PACS numbers: 73.63.Fg, 73.61.Wp

Carbon nanotubes are potentially the smallest building blocks for future generation electronic devices [1,2]. Rational design of any device requires a fundamental understanding of the electronic properties, of which single-wall nanotubes (SWNTs) have been well understood. Consequently, electronic devices such as field-effect transistors [3,4], nanotube-nanotube junctions [5,6], and integrated logic circuits based on SWNTs [7–9] have been realized. In contrast, understanding transport properties of multiwall nanotubes (MWNTs) has proceeded more slowly because of their extremely complex structure. A MWNT consists of many nested SWNTs in which each has a different electronic structure. All the transport studies carried out so far use a ''side contact'' [10] in which nanotubes are spread on a prepatterned Au electrode, with only the outmost wall contacted to the electrodes, and the inner carbon walls being not in direct contact with the electrodes. As such, parallel conduction paths along the inner walls are limited in their contribution to the overall conductance [11–13]. Indeed, experiments have shown that current flows only in the outmost wall in side-contacted MWNTs [11,14]. Collins *et al.* [15,16] attempted to characterize the conductivity of *side-contacted* MWNTs by using an electric breakdown technique. Their results are promising but are complicated by the tunneling barrier due to the side-contact geometry. Here we report the realization of an *end-contact* geometry [10], in which every wall of the MWNTs is contacted by the electrodes. This is a more generic contact configuration for the study of transport in multilayer systems. Consequently, we were able to reveal the transport properties of each wall within a MWNT.

Our experimental setup is shown in Figs. 1(a) and 1(b). A MWNT is end contacted and free standing in high vacuum (10^{-8} Torr), inside a high-resolution transmission electron microscope (HRTEM) equipped with a scanning tunneling microscopy (STM) probe. In such an arrangement, atomic-scale imaging and *I-V* measurements were carried out concurrently for the first time. Figure 1(b) shows a MWNT grown on a carbon fiber by chemical vapor deposition. A contact was made on the left between a STM probe (not shown) and the nanotube tip by the deposition of amorphous carbon using electron beam radiation. When applying a bias of about 2 V, the catalyst particle on the nanotube tip is molten and moves rapidly toward the STM probe. The encapsulated nanotube tip is broken after the catalyst particle passes through, leaving each wall being contacted by the amorphous carbon or the STM probe. On the other end of the nanotube, each wall is contacted to the carbon fiber because of the tip growth mechanism [17].

The electronic properties of each wall are probed using the electric breakdown method [15,16]. When passing a current of 240 μA, breakdown occurs at the midpoint of the nanotube, resulting in the formation of a clean six-wall nanotube segment, which was eliminated wall-by-wall by electric breakdown. The loss of one wall under a constant bias of 3 V results in an instant current drop, as shown in Fig. 1(c). The current drops are approximately 13, 17, 25, and 31 μA for the 6th, 5th, 4th, and 3rd wall breakdown (the innermost wall is labeled as the first wall), respectively. The sequential wall-by-wall breakdown was recorded by HRTEM in our experiments. Figure 2 shows clearly that one wall is removed after each current drop, and each wall is removed sequentially from the outermost wall (6th) to the innermost wall (2nd). HRTEM indicates that the breakdown eventually results in the formation of either a double-wall nanotube or a SWNT junction. Remarkably, HRTEM detects that each breakdown is initiated in the *middle* of the nanotube, *not* at the contact (Figs. 2–4, [18]).

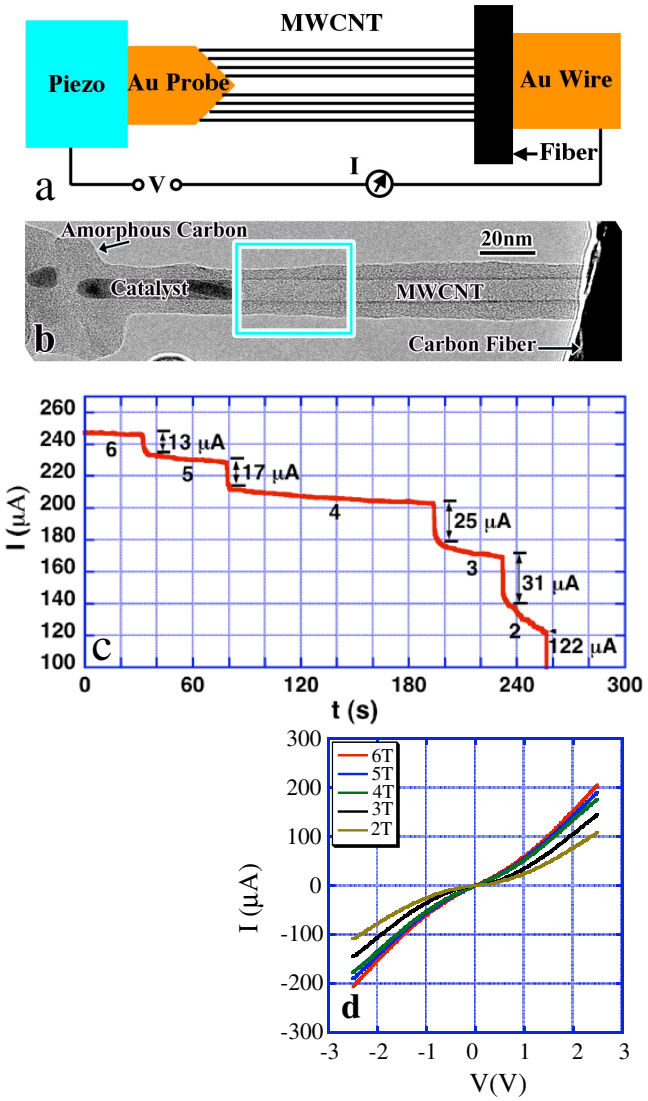

FIG. 1 (color online). (a) and (b) show that a MWNT grown on a carbon fiber was side contacted by a STM probe, which is further attached to a piezomanipulator. The carbon fiber is glued to a gold wire. The MWNT in (b) has a catalyst particle on the tip. The frame in (b) indicates the location of the breakdown. (c) The current-time (I-t) curve of the breakdown of the MWNT shown in panel (b) and Fig 2. The numbers below the plateau indicate the total wall number. (d) I-V plots of the MWNT shown in Fig. 2. 6 T, . . . , 2 T denote the total number of walls being 6, . . ., 2, respectively.

Intuitively, the wall-by-wall breakdown may occur sequentially from the outer to innermost walls. Surprisingly, our HRTEM reveals that this (Fig. 2) is only one of the three possible burning patterns. The breakdown can proceed alternatively between the outer and the inner walls. Figure 3 shows the breakdown of a five-wall nanotube. Initially, a hole is formed on the surface of the outermost wall [Fig. 3(a), [18]]. After 5 min, the entire wall is broken with the residue shown in Fig. 3(b). This triggers a current drop of 8 μA [Fig. 3(e)]. Surprisingly, the next breakdown occurs from the innermost wall [Fig. 3(c)]. Remarkably, we found a large current drop of 24 μA once the inner wall is broken, proving unambiguously that the inner wall is carrying a significant amount of current. The third breakdown also occurs from the inside [Fig. 3(d)], causing another 24 μA current drop. It should be noted that all

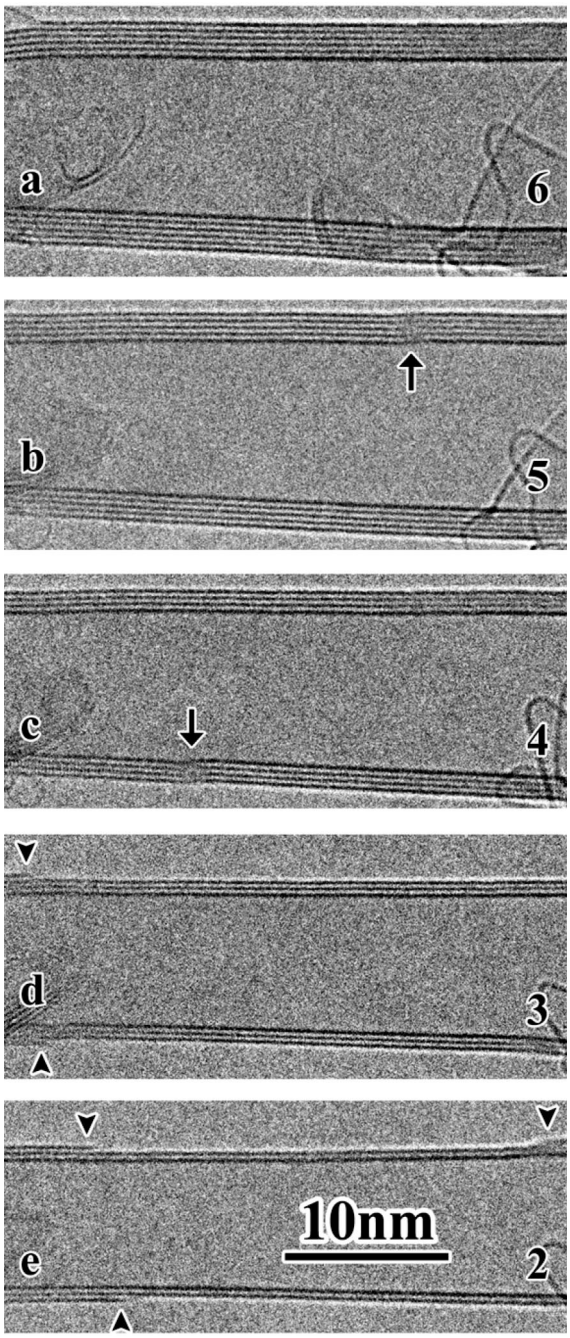

FIG. 2. Sequential HRTEM images showing that the six-wall nanotube is removed wall-by-wall from the outermost wall (a) to the innermost wall (e). The numbers indicate the total number of walls. The arrows mark kinks. The arrowheads denote the residue of the 4th and the 3rd walls after breakdown.

the breakdowns are initiated in the middle of the clean MWNT segment.

Figure 4 presents the third observed behavior in which the breakdown takes place sequentially from the innermost wall (1st) to the outermost wall (4th), completely reversing the burning sequences observed in the nanotube shown in Fig. 2, until a SWNT is formed. The current drops are 6, 12, and 14 μA for the 1st, 2nd, and 3rd wall breakdown [Fig. 4(f)], respectively. It is interesting to note the interplay between the wall-diameter dependence of the current drop and the breakdown sequence. Figure 4 shows that the amount of current drop increases with increasing wall diameter, consistent with the results of Bourlon *et al.* [19], but opposite to what is shown in Fig. 2, where the breakdown starts from the outmost wall.

We now turn to the transport properties for the MWNT displayed in Fig. 2. The *I-V* curves [Fig. 1(d)] maintain a similar profile following each breakdown: at low bias, they are linear, suggesting that the transport and the contacts are Ohmic. The resistances extracted from the linear *I-V* curve vary from 21 kΩ for 6 T to 108 kΩ for 2 T at room temperature. The resistivities vary from 788 to

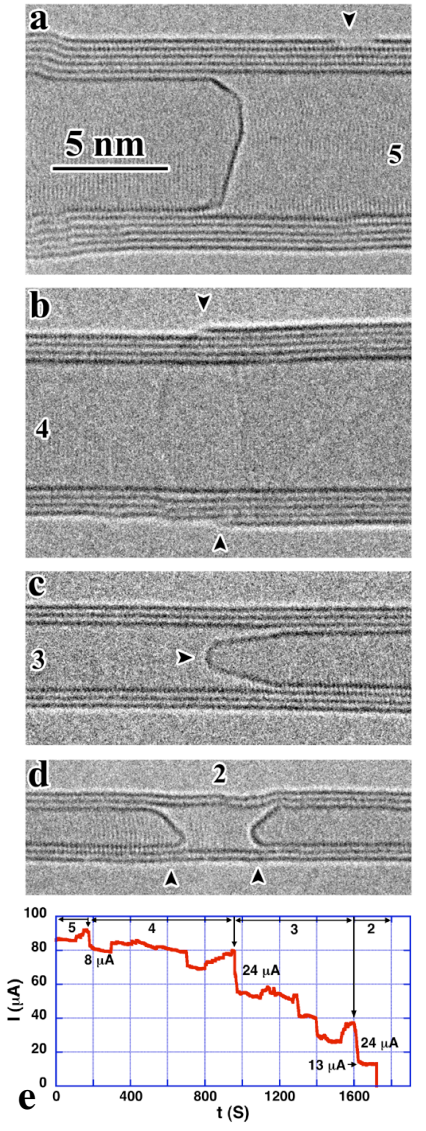

FIG. 3 (color online). A MWNT breaking in a sequence alternatively between the outermost wall and innermost wall. The numbers mark the number of walls in the broken segments. The arrowheads denote the breaking locations. The vertical arrows in (e) mark the current drop when a wall is removed. The outermost wall opens a hole (a) and breaks completely (b). The innermost wall is broken (c), and the second innermost wall is broken (d). (e) The *I-t* curve.

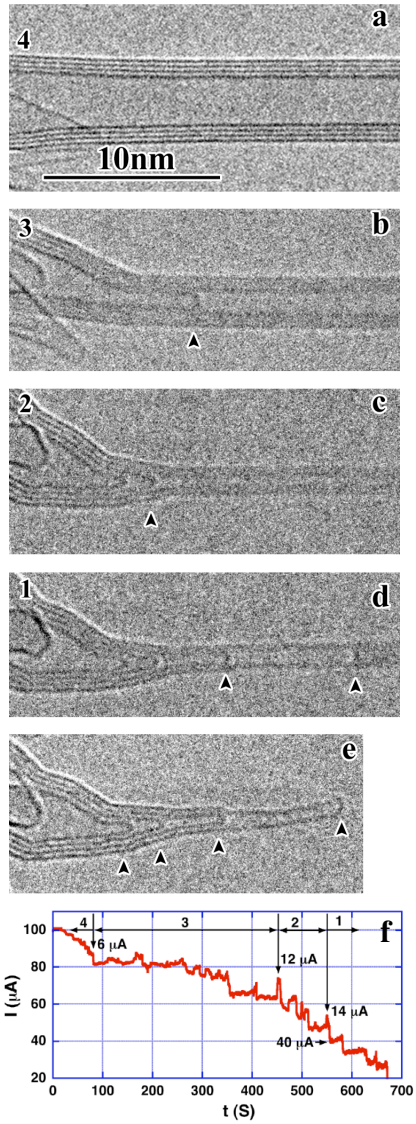

FIG. 4 (color online). The four walls of the MWNT in (a) are sequentially removed from the innermost to the outermost wall [(b) to (d)]. (e) The residue of the four broken walls. (f) The *I-t* curve. The numbers mark the total number of walls in the broken segments. The arrowheads denote the breaking locations. The vertical arrows in (f) mark the current drop when one wall is removed.

1345 $\mu\Omega$ cm, which is comparable to that reported by Dai *et al.* [20]. At higher bias, the *I-V* curves become nonlinear. However, up to the breakdown voltage of 3 V, we did not observe *apparent* current saturation as reported by others [15,16,19,21]. The current saturation has been attributed to backscattering by optical phonons [21] and interband Zener tunneling [19]. And it is pushed to higher voltages in our large diameter MWNTs because of the change in the phonon spectrum and the relatively short tube length (about 200 nm).

We now turn our focus to the breakdown mechanism. The observation (Figs. 2–4) that the breakdown is initiated in the middle of the nanotube (not in the contacts) indicates that it is caused by resistive heating. This is also supported by the defect generation and migration along the nanotubes. Typical defects observed are kinks (Fig. 2), holes [18], and sliding between different walls [18]. These are apparently heat-stimulated imperfections. From the lattice spacing of 4 Å, we estimate that the temperature in the middle of nanotube is between 2000 and 3000 °C at the breakdown voltage of 3 V. From the Fourier law, the middle section of the nanotube is the hottest spot; therefore it is not difficult to understand that the breakdown occurs in the middle of the nanotube, starting either from the outermost wall or from the innermost wall.

These observations naturally imply that the transport in the MWNTs is not ballistic and that significant scattering occurs as carriers traverse the length of the nanotubes. To this end, an estimate of the carrier mean free path (λ_{MF}) is useful. From the Einstein relation, the conductance is given by $G = (\pi dm/L)e^2 D\nu$, where d is the averaged tube diameter, m is the number of walls, L is the length of the nanotube between the end contacts, $D = V_{\mathrm{F}}\lambda_{\mathrm{MF}}/2$ is the diffusion constant, and $\nu = 2\Delta E/\pi(\hbar V_{\mathrm{F}})^2$ is the density of states, where V_{F} is the Fermi velocity and ΔE is the energy measured from the Fermi level which we replace with the thermal energy $k_B T$ at room temperature. The mean free path is thus given by $1/\lambda_{\mathrm{MF}} = \pi dm\rho G_0(k_B T/\hbar V_{\mathrm{F}})$, with $\rho = R/L$ the resistance per unit length and $G_0 = 2e^2/h = 1/(13\ \mathrm{k}\Omega)$. Using the experimental values $m = 6$, $R = 20\ \mathrm{k}\Omega$, $d = 12$ nm, and the length of the nanotube $L = 200$ nm, we obtain an averaged $\lambda_{\mathrm{MF}} = 13$ nm, which agrees excellently with that reported by Javey *et al.* [22]. Since the averaged mean free path is much shorter than the length of the nanotube, the transport is diffusive and electron heating is unavoidable at large bias and power input. Although we observed defect generation and migration in the nanotube walls under high bias conditions, and the breakdown might be initiated from the defect site, the defects were found to emerge and then disappear from anywhere in the nanotube randomly; therefore, this cannot account for our results that the breakdown always starts from the middle of the nanotube. We conclude that the middle part of the nanotube is the hottest spot, and the transport in our nanotube is diffusive rather than ballistic.

The work is sponsored by DOE DE-FG02-00ER45805 (S. C., S. H. J., and Z. F. R.), DE-FG02-99ER45747 (Z. W.), and DE-FG02-02ER45977 (G. C.), and by NSF NIRT 0304506 (Z. F. R.), MRI 0320177 (J. Y. H. and Z. F. R.), and DMR-04-05538 (M. S. D.).

*Corresponding author.
†Electronic address: huangje@bc.edu
‡Electronic address: renzh@bc.edu

[1] C. Dekker, Phys. Today **52**, No. 5, 22 (1999).
[2] M. S. Dresselhaus, G. Dresselhaus, and P. Avouris, *Carbon Nanotubes: Synthesis, Structure, Properties, and Applications* (Springer, Heidelberg, 2001).
[3] S. J. Tans, A. R. M. Verschueren, and C. Dekker, Nature (London) **393**, 49 (1998).
[4] R. Martel *et al.*, Appl. Phys. Lett. **73**, 2447 (1998).
[5] M. S. Fuhrer *et al.*, Science **288**, 494 (2000).
[6] Z. Yao, H. W. C. Postma, L. Balents, and C. Dekker, Nature (London) **402**, 273 (1999).
[7] A. Bachtold, P. Hadley, T. Nakanishi, and C. Dekker, Science **294**, 1317 (2001).
[8] V. Derycke, R. Martel, J. Appenzeller, and P. Avouris, Nano Lett. **1**, 453 (2001).
[9] X. Liu, C. Lee, C. Zhou, and J. Han, Appl. Phys. Lett. **79**, 3329 (2001).
[10] J. J. Palacios *et al.*, Phys. Rev. Lett. **90**, 106801 (2003).
[11] S. Frank, P. Ponchral, Z. L. Wang, and W. A. De Heer, Science **280**, 1744 (1998).
[12] C. Schönenberger *et al.*, Appl. Phys. A **69**, 283 (1999).
[13] S. Roche, F. Triozon, A. Rubio, and D. Mayou, Phys. Lett. A **285**, 94 (2001).
[14] A. Batchtold *et al.*, Nature (London) **397**, 673 (1999).
[15] P. G. Collins, M. S. Arnold, and Ph. Avouris, Science **292**, 706 (2001).
[16] P. G. Collins, H. Hersam, M. Arnold, R. Martel, and P. Avouris, Phys. Rev. Lett. **86**, 3128 (2001).
[17] M. Endo, R. Saito, M. S. Dresselhaus, and G. Dresselhaus, in *From Carbon Fibers to Nanotubes*, edited by T. W. Ebbesen (CRC Press, Inc., London, 1997).
[18] See EPAPS Document No. E-PRLTAO-95-042552 for sequential HRTEM images showing the breakdown of the 5th wall of the nanotube shown in Fig. 2 and HRTEM movies of Figs. 2 and 3. A direct link to this document may be found in the online article's HTML reference section. The document may also be reached via the EPAPS homepage (http://www.aip.org/pubservs/epaps.html) or from ftp.aip.org in the directory /epaps/. See the EPAPS homepage for more information.
[19] B. Bourlon *et al.*, Phys. Rev. Lett. **92**, 26 804 (2004).
[20] H. Dai, E. W. Wong, and C. M. Lieber, Science **272**, 523 (1996).
[21] Z. Yao, C. L. Kane, and C. Dekker, Phys. Rev. Lett. **84**, 2941 (2000).
[22] A. Javey, J. Guo, Q. Wang, M. Lundstrom, and H. J. Dai, Nature (London) **424**, 654 (2003).